J Mol Model (2015) 21: 181
DOI 10.1007/s00894-015-2719-9

ORIGINAL PAPER

# Effects of alloying on oxidation and dissolution corrosion of the surface of γ-Fe(111): a DFT study

**Cheng Han [1,2] · Caili Zhang [1,2] · Xinglong Liu [1,2] · Hui Huang [1,2] · Shengyi Zhuang [1,2] · Peide Han [1,2] · Xiaolei Wu [3]**

Received: 19 March 2015 / Accepted: 1 June 2015 / Published online: 27 June 2015
© Springer-Verlag Berlin Heidelberg 2015

**Abstract** Effects of alloying elements in popular steels on the oxidation and dissolution corrosion of the surface of γ-Fe(111) have been investigated by performing density functional theory calculations within the local density approximation. First, the segregation of alloying atoms as well as preferential adsorption sites for oxygen and water were carefully examined, and it was found that all of the alloying elements considered had a tendency to segregate to the surface, and that the most preferred adsorption sites were the hexagonal closed packed (hcp) site and the top site for oxygen and water, respectively. The adsorption energies that characterized the tendency for oxygen or water to be adsorbed on the alloy surface showed that all ten alloying elements (especially Cr, Si, and Cu) were able to inhibit the adsorption of oxygen, and that all of the alloying elements except for Nb, Mo, and Ti inhibited water adsorption. The electrode potentials, which indicate the electrochemical stabilities of the surfaces of the alloys, suggested that all of these alloying elements (especially Cr, Mo, and Si) were able to suppress the adsorption of oxygen and water on the investigated surfaces, except for Nb and Ti in the case of water adsorption. Density of states analysis further indicated that all ten alloying elements (especially Cr, Si, Mo, and Cu) enhanced the corrosion resistance of the fcc Fe substrate, except for Nb and Ti with respect to dissolution corrosion.

**Keywords** γ-Fe · Oxidation · Dissolution corrosion · Adsorption · Electrode potential · First-principles study

✉ Caili Zhang
zcl2016@126.com

✉ Peide Han
hanpeide@126.com

[1] College of Materials Science and Engineering, Taiyuan University of Technology, No. 79 West Yingze Street, Taiyuan 030024, People's Republic of China

[2] Key Laboratory of Interface Science and Engineering in Advanced Materials of Taiyuan University of Technology, Ministry of Education, Taiyuan 030024, China

[3] State Key Laboratory of Nonlinear Mechanics, Institute of Mechanics, Chinese Academy of Sciences, Beijing 100080, China

## Introduction

Iron-based alloys are widely used in modern industrial applications due to the abundant raw resources for such alloys in the natural world, their low cost, and their good mechanical and processing properties. However, they can easily corrode over time, which is a critical issue during the development of new alloys. Globally, the technological and economic losses caused to industry by corrosion soak up 3~4 % of the annual GDP, which has led to intensive efforts to minimize its adverse effects. Although new stainless steels with greatly improved abilities to resist corrosion have been created by adding different proportions of alloying elements to the iron, localized corrosion may still take place due to the activity of Fe and damage to or even removal of the passive film on the alloy surface, which is mainly composed of an Fe-Cr spinel and magnetite [1–3], under certain conditions. Local etching such as pitting and galvanic corrosion impact alloy performance significantly. Therefore, it is necessary to understand the impact of alloying elements on the corrosion of clean surfaces without their native oxide films in order to alleviate the adverse effects of alloying that occur under special conditions.

It is known that the corrosion of structural materials is related to surface adsorption and other chemical reactions that happen in certain corrosive environments. Oxygen or water adsorption on transition metal surfaces is crucial to various surface processes such as oxidation, corrosion, and

heterogeneous catalysis [4, 5]. Chemical attack on a metal surface is boosted by the adsorption of water, as it can provide favorable conditions for a variety of surface reactions. Thus, the adsorption of oxygen or water on single-crystal surfaces has long been an issue of intense study and debate. Due to the economic impact of corrosion, experimental investigations of [6–8] and theoretical predictions for [9–13] the reactivity of iron have received a great deal of attention. For instance, the oxidation of Fe-Cr alloys has been investigated experimentally using Mossbauer and X-ray photoelectron spectroscopy [8], while the adsorption of oxygen and water on ferritic stainless steel (Fe-17Cr) has been studied by X-ray photoelectron spectroscopy (XPS) and inelastic electron background analysis [14]. Important examples of theoretical studies include those that have used density functional theory (DFT) calculations to explore the adsorption of oxygen on Fe(110) and (100) surfaces [15], water dissociative adsorption and aggregation on the Fe(100) surface [16], the initial corrosion of an iron surface [12], and the influence of liquid metals on the dissolution corrosion of an iron surface [17].

There are two crystal structures of iron: ferrite/α,δ-Fe with a body-centered cubic (bcc) structure and austenite/γ-Fe with a face-centered cubic (fcc) structure. Although significant efforts have been made over the last few decades to study the corrosion of iron surfaces, most of these experimental and theoretical works have focused on α-Fe (bcc) [18–22]. Theoretical studies of γ-Fe (fcc) have also been performed [23–25], including a few on the effects of alloying on an fcc Fe surface that is adsorbing oxygen or water. Such works can help guide the selection of appropriate corrosion inhibitors for duplex stainless steels and austenitic steels, which play important roles in industry.

In the work reported in the present paper, we focused our attention on the effects of alloying on the corrosion-related properties of an ideal native γ-Fe surface during oxygen or water adsorption. First-principles calculations were carried out to study the effects of ten common alloying elements (Cr, Si, Cu, Al, Ni, Nb, Co, Mo, Mn, Ti) on the adsorption of oxygen or water and the change in the electrode potential at the surface of each Fe-M (M = Cr, Si, Ti, Mo, Nb) alloy. Both of these aspects are related directly to the corrosion properties of the alloys. Such a computational method has previously been successfully used to interpret experimental results, predict properties, and even to design materials. We hope that the results of this study will lead to an understanding of the fundamental atomic-scale mechanism behind the role of alloying elements in the resistance of native austenite to corrosion.

## Model and methods

Density functional theory (DFT) [26, 27] calculations were performed using the CASTEP code (Cambridge Sequential Total Energy Package) [28] in the framework of the local density approximation (LDA). The Ceperley–Alder–Perdew–Zunger (CA-PZ) functional [29, 30] was employed as the exchange-correlation functional. The Hellmann–Feynman forces were minimized to determine the ground-state atomic geometry. Brillouin zone integration was performed using a [5×5×1] k-point mesh generated via the Monkhorst–Pack scheme [31]. A cutoff energy of 350 eV was used throughout. In order to achieve a good compromise between calculation accuracy and efficiency, face-centered cubic slabs that consisted of a periodic array of seven Fe layers and were separated by 10-Å-thick layers of vacuum (to ensure that there was no significant interaction between the slabs) were modeled, and a (2×2) lateral cell of the nonmagnetic fcc Fe(111) surface was simulated (see Fig. 1). We optimized the coordinates of the top three atomic layers of the slab and adsorbates, while the positions of the bottom four layers of Fe atoms were fixed at their positions in bulk. Full relaxation of atomic positions was carried out until the forces on each atom had converged to less than 0.05 eV/Å. This set of parameters permits a self-consistent field convergence tolerance of up to $2\times10^{-6}$ eV/atom.

In order to ensure that the calculations performed were reliable, the lattice parameter of bulk fcc Fe was calculated using both the LDA and the GGA functionals (a comparison with values given in [32] is provided in Table 1). The calculated values indicate that the lattice constant value obtained using the LDA is more consistent with the result given in [32], and lies between the known experimental value of 0.365 nm [33] and the value obtained using the GGA. Therefore, the LDA was applied in the following surface relaxation and energy calculations. Although our calculated lattice parameter value (0.345 nm) is very close to some previously reported values of 0.345 nm [32] and 0.343 nm [34], there are discrepancies from other theoretical values (0.359 nm [35] and 0.364 nm [36]) and an experimental value (0.365 nm [33]). These differences are caused by the use of different calculation methods and parameter settings in those works. Note that all of the energies (segregation energy, adsorption energy, and electrode potential) considered here are relative values that are obtained by calculating the differences between absolute values (all of these relative values are less than their corresponding experimental values), thereby diminishing the relative tolerance provided by a same parameters settings. Also, using our method, the length of the O–H bond and the bond angle H–O–H were found to be 0.978 Å and 105.4°, respectively, which are in good agreement with the corresponding experimental values of 0.958 Å and 104.5° [37], as well as some other theoretical values (0.978 Å and 104.3°, respectively [38]), thus demonstrating that our calculation is reliable.

In the present adsorption calculations, the water molecule was aligned parallel to the surface. As the stacking order along the [111] lattice direction is ABC and all the alloying elements

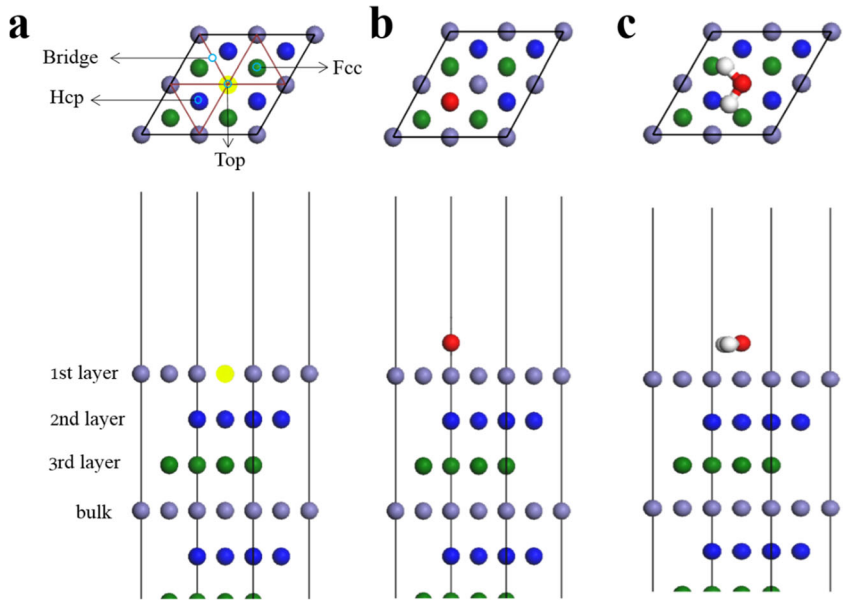


**Fig. 1** **a**–**c** Computational models of the adsorption surface, showing top and side views (partial) along with **a** all possible adsorption sites (hcp, fcc, bridge, and top) and **b**, **c** the most stable sites for oxygen and water adsorption, respectively, on the fcc Fe(111) surface. The *red* and *white balls* represent oxygen and hydrogen atoms, respectively; *green circles* indicate possible adsorption sites; other colors (*gray*, *blue*, *green*) are used to show the different layers of Fe atoms; the *yellow ball* indicates a site at which an alloying atom was substituted

considered here show topmost surface segregation, there are four possible adsorption sites on the surface. Adsorbed species were placed either directly on top of the central Fe on the surface (top site), between two Fe atomic bonds (bridge site), at the center of a hollow region in the second layer of atoms, directly above (fcc site), or at the center of a hollow region in the third layer of atoms, directly above (hcp site) (see Fig. 1). For all of the Fe-M alloys considered here, the central Fe atom on the surface was substituted by an alloying atom, and $H_2O$ or O was placed near to the alloying atom.

## Results and discussion

### Segregation of alloying atoms on the fcc Fe(111) surface

We know that an alloying atom or impurity has a tendency to segregate to or away from the surface in order to achieve a stable state by minimizing its total energy, which can considerably modify the properties of the surface. So, it is very important to examine this surface segregation before investigating the effects of different alloying elements on the adsorption of oxygen or water on the fcc Fe surface.

In the present work, the segregation properties of ten common alloying elements were examined. The surface segregation energy (SE) of alloying atom M is defined as [39]

$$E_{\text{seg}}^{\text{M}} = E_i^{\text{M}} - E_{\text{bulk}}^{\text{M}} \quad (1)$$

where $E_{\text{bulk}}^{\text{M}}$ is the total energy of the supercell containing M at the bulk site (in our case in the fifth layer of the slab), and $E_i^{\text{M}}$ is the total energy of the slab with M moved to the $i$-th layer from the surface ($i$ = 1, 2, 3, 4). A negative/positive $E_{\text{seg}}^{\text{M}}$ means that M does/does not segregate to the $i$-th layer from the surface. The calculated segregation energies are displayed in Fig. 2 as a function of layer depth.

For all of the alloying elements considered except for Cr, the segregation energies in the surface and subsurface layers showed the same tendency for the SE to be negative in the surface layer and positive in the subsurface layers. This obviously suggests that the alloying elements considered here tend to segregate to the surface, except for Cr, which seems to prefer to be in a subsurface layer. According to previous studies, this anomalous segregation of Cr also occurs in bcc Fe, which can be attributed to a complex interaction involving the antiferromagnetism of Cr and the ferromagnetism of bcc Fe [40–42]. Discerning the reason for the anomalous Cr segregation on the fcc Fe(111) surface may require further study of the paramagnetic phase of fcc Fe. However, it has been pointed out that the segregation of Cr depends strongly on its concentration, indicating that segregation to the surface layer may occur as the concentration of Cr is increased [39, 43]. We confirmed this hypothesis by calculating another slab with a higher Cr concentration, which gave results in agreement with the previous bcc Fe results. The surface segregation of Cr was also confirmed in experiments performed using the CEMS technique [8]. Based on these segregation results, we only

**Table 1** Lattice parameters of fcc Fe obtained using both LDA and GGA functionals

| Parameter | LDA | GGA-PW91 | GGA-PBE | From [32] |
|---|---|---|---|---|
| $a$ (Å) | 3.454 | 3.446 | 3.447 | 3.45 |
| $V$ (Å$^3$) | 41.21 | 40.88 | 40.93 | 41.2 |

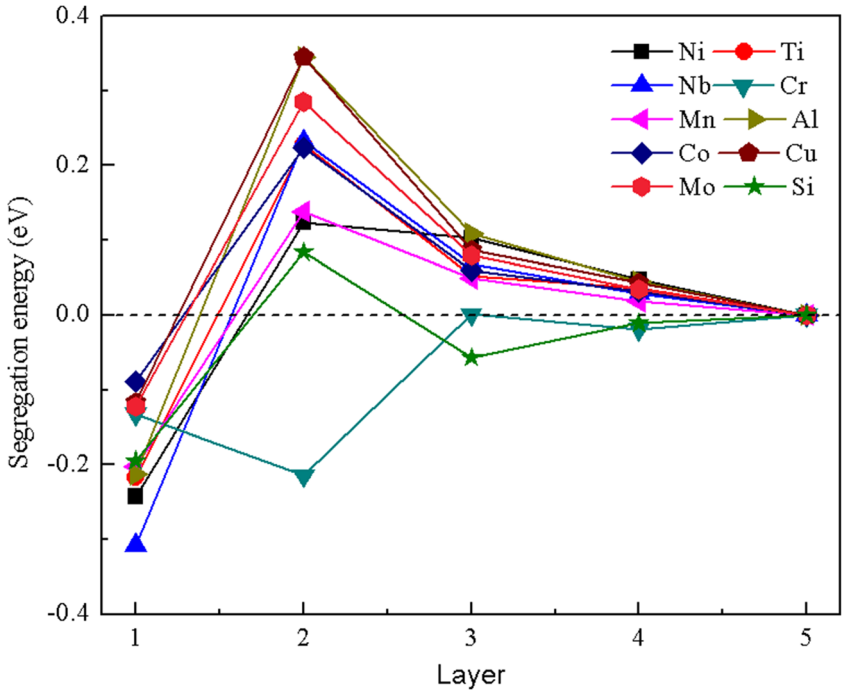


**Fig. 2** Segregation energies calculated for alloying atoms in different surface and subsurface layers of fcc Fe(111)

considered alloying atoms in the topmost layer in subsequent investigations.

### Adsorption of O and $H_2O$ on a clean fcc Fe surface

The adsorption energies of oxygen and water on a clean fcc Fe(111) surface were calculated according to the following formula [15]:

$$E_{ads} = E_{slab}^{ads} - E_{slab} - E_{tot}^{ads} \quad (2)$$

where $E_{slab}^{ads}$ and $E_{slab}$ are the total energy of the Fe slab with and without the adsorbed species on the surface, respectively, and $E_{tot}^{ads}$ is the total energy of the adsorbed species. Thus, a negative value of $E_{ads}$ implies that the adsorption of the species is thermodynamically favorable.

As shown in Table 2, for oxygen, the adsorption energy is lowest (−12.44 eV) at the hcp site, followed by the fcc site (−12.08 eV), demonstrating that the most stable adsorption site for oxygen on the surface is hcp, and the type of adsorption that occurs is chemisorption. Meanwhile, the calculated results for water adsorption suggest that initial configurations in which adsorption occurs at the hcp, fcc, and bridge sites eventually convert into the top site configuration, indicating that the most stable adsorption site for water is the top site. Furthermore, the adsorption energies of oxygen and water on alloying-atom-doped γ-Fe(111) surfaces were also examined, which yielded similar results to those seen for the clean surface. This indicates that the introduction of these alloying atoms does not change the relative stabilities of the potential sites for oxygen or water adsorption on the alloy surfaces. Considering that the structure of the surface barely changes with the introduction of an alloying atom, the hcp site and top site were chosen as the adsorption sites for oxygen and water, respectively, in subsequent calculations.

### $H_2O$ and O adsorption on doped surfaces

We then turned our attention to the effects of alloying on adsorption. Introducing an alloying atom into the surface can either enhance or reduce the adsorption of water and oxygen on the surface. We analyzed the effects of alloying on adsorption by calculating the adsorption energy ($E_{ads}$) along with the binding energy ($E_b$), which characterize how easily oxygen or water is adsorbed on the alloy surface as well as the interactions between the adsorbates and the alloying atoms. $E_{ads}$ was

**Table 2** Adsorption energies of both oxygen and water at four possible adsorption sites on the pure fcc Fe(111) surface and the final configuration the system in each case

| | Initial configuration | $E_{ads}$ (eV) | Final configuration |
|---|---|---|---|
| Oxygen | Top | Unstable | Hcp |
| | Bridge | Unstable | Hcp |
| | Hcp | −12.44 | Hcp |
| | Fcc | −12.08 | Fcc |
| Water | Top | −3.37 | Top |
| | Bridge | Unstable | Top |
| | Hcp | Unstable | Top |
| | Fcc | Unstable | Top |

calculated using Eq. 2 and $E_b$ was calculated by the following formula:

$$E_b = E_{slab}^{AA+ads} + E_{slab} - E_{slab}^{ads} - E_{slsb}^{AA} \quad (3)$$

where $E_{slab}^{AA+ads}$ and $E_{slsb}^{AA}$ are the total energies of the corresponding slab with and without the adsorbate on the alloying-atom-doped surface. A negative binding energy indicates the presence of an attraction between the adsorbed species and the alloying atom, while a positive binding energy implies repulsion. The larger the absolute value of $E_b$, the stronger the interaction between the adsorbed species and the alloying atom.

The calculated $E_{ads}$ and $E_b$ values of oxygen and water on these alloy surfaces are displayed in Figs. 3 and 4, respectively. For oxygen adsorption, the $E_{ads}$ and $E_b$ values on the alloying-atom-doped surfaces increase in the following order: clean Fe < Ti < Mn < Mo < Co < Nb < Ni < Al < Cu < Si < Cr. The higher adsorption energies of the alloying-atom-doped surfaces compared to pure iron indicate that oxygen adsorption is inhibited by the introduction of an alloying atom, which mitigates the surface oxidation of the alloy to some degree. For water adsorption, the order of adsorption energies with respect to alloying atom is similar to that for oxygen adsorption, except for Ti, Mo, and Nb. Thus, the presence of an alloying atom led to a reduction in water adsorption except in the cases of Ti, Mo, and Nb, which enhance the adsorption of water given their lower $E_{ads}$ and $E_b$ values than those of the clean Fe surface. It was also found that, among all ten of the alloying elements considered, Cr enhances the ability of the surface to resist oxygen or water adsorption to the greatest degree, followed by Si and Cu.

We also reach the same conclusion upon considering the geometry of the adsorption system. As shown in Table 3, the distance between $H_2O$ and the alloy surface shows a similar trend with respect to alloying element to those seen for $E_{ads}$ and $E_b$: introducing Nb, Ti, or Mo causes the water molecule to approach more closely to the surface, whereas introducing Cr or Si has the opposite effect. Meanwhile, introducing any of the alloying elements causes the distance between the subsurface and topmost surface layers to increase, and the Fe–M distance in the alloys is always larger than the Fe–Fe distance in pure Fe. The adsorption energies and trends in distances between atoms and layers indicate that chemisorption of water occurs on these surfaces, and the introduction of an alloying atom influences surface adsorption because it interacts with the other atoms in the surface matrix.

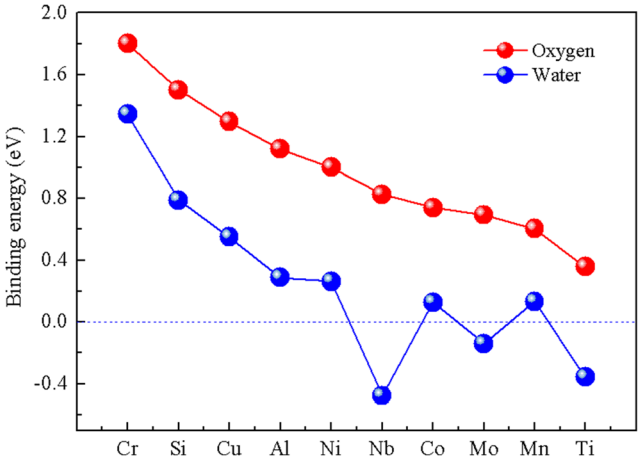


**Fig. 4** Binding energies of oxygen and water to various alloying-atom-doped surfaces

## Electrochemical potential shift

Aside from the adsorption energy, we also looked at the impact of alloying elements on the interaction between the adsorbed species and the adsorbing surface in more depth by considering the electrochemistry of the system. The

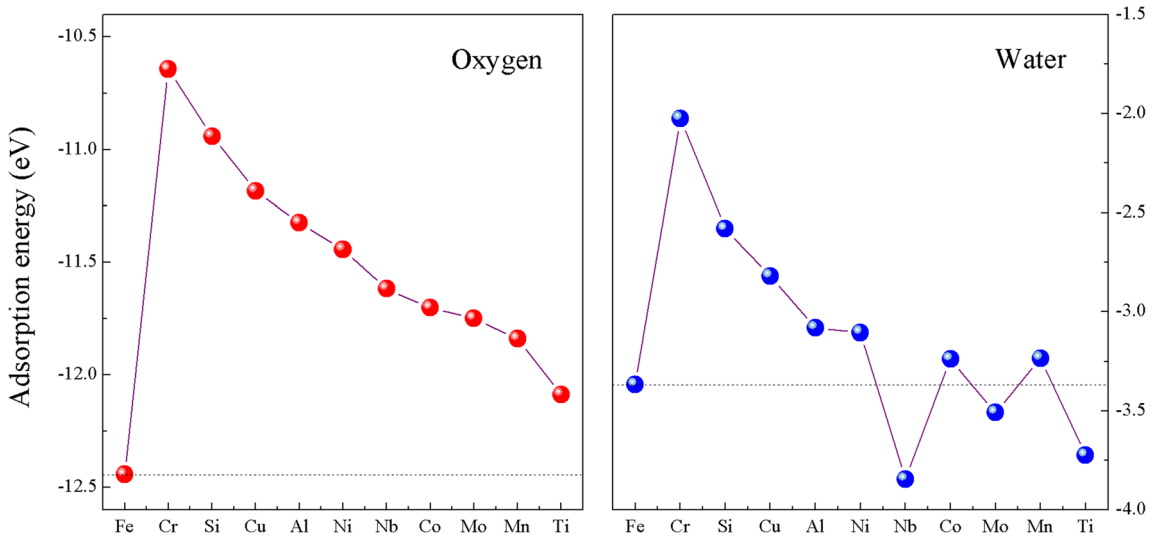


**Fig. 3** Adsorption energies for oxygen and water on various alloying-atom-doped surfaces

**Table 3** Optimized structural parameters for the adsorption of oxygen and water on surfaces of pure Fe and various alloys

| Surface | Oxygen | | | Water | | |
|---|---|---|---|---|---|---|
| | $d_{Fe–M}$ (Å) | $d_{O–surface}$ (Å) | $d_{top–sub}$ (Å) | $d_{Fe–M}$ (Å) | $d_{H2O–surface}$ (Å) | $d_{top–sub}$ (Å) |
| Pure Fe | 2.25 | 1.08 | 1.91 | 2.35 | 2.04 | 1.78 |
| Fe-Cr | 2.26 | 1.12 | 1.92 | 2.38 | 2.07 | 1.85 |
| Fe-Si | 2.33 | 1.11 | 1.91 | 2.43 | 2.10 | 1.85 |
| Fe-Nb | 2.36 | 1.11 | 1.92 | 2.46 | 1.93 | 1.86 |
| Fe-Mo | 2.32 | 1.10 | 1.92 | 2.41 | 2.03 | 1.84 |
| Fe-Ti | 2.39 | 1.12 | 1.93 | 2.44 | 1.96 | 1.83 |

adsorption of oxygen or water on the metal surface causes the surface potential of the alloy to change, thus influencing the electrode potential of the system [22]. Considering that the alloying elements considered here had different effects on water adsorption by the alloy, and to probe the impact of Ti, Mo, and Nb on the surface corrosion properties in more detail, the electrode potential shifts $\Delta U$ of Fe-M (M = Cr, Si, Ti, Mo, Nb) alloy surfaces with respect to the pure fcc Fe surface for the reaction $Fe^{2+}+2e=Fe$ were calculated using the formula

$$\Delta U = U_{Fe–M} - U_{Fe} \tag{4}$$

in which $U_{Fe-M}$ and $U_{Fe}$ are the electrode potentials of the Fe atoms in Fe-M and in the pure fcc Fe(111) surface relative to the standard hydrogen electrode, respectively. The electrode potential can be calculated as follows [44, 45]:

$$U = \frac{\Delta G}{nF} \propto \frac{\mu}{n} \approx \frac{E_{slab} - E'_{slab}}{2e} \tag{5}$$

where $E_{slab}$ and $E'_{slab}$ are the total energy of the slab with and without a Fe atom removed from the slab, respectively, and $\mu$ is the chemical potential of an Fe atom in the slab, which can be evaluated approximately by calculating the difference in total energy between the optimized original slab and new slab with vacancies.

It should be noted that since $E'_{slab}$ varies depending on the position of the Fe atom removed, we evaluated the chemical potentials using slabs with Fe removed at the same position. Using this approach, the positive/negative electrode potential shift $\Delta U$ indicates the rise/decline of the electrode potential of the Fe-M surface relative to the pure Fe surface, allowing us to determine if the introduction of alloying element M leads to a higher/lower ability of the surface to resist being electrochemically corroded.

As shown in Table 4, for oxygen adsorption, there is strong agreement between the results of the present calculations and the results of previous $E_{ads}$ calculations; that is, the introduction of an alloying atom not only mitigates oxygen adsorption but it also increases the electrode potential of the alloy surface. For water adsorption, the electrode potential shifts ($\Delta U$) of Cr, Si, Nb, Mo, and Ti with respect to that of the pure Fe surface vary. The $\Delta U$ values of Cr, Si, and Mo are positive and decrease in the order Mo > Cr > Si, meaning that these alloying elements suppress the removal of Fe atoms from the surface, making the alloy surface less susceptible to electrochemical corrosion than the pure Fe surface. On the other hand, the presence of the alloying elements Nb and Ti encourages the dissolution of Fe atoms, as their electrode potential shifts are negative, indicating that they facilitate surface erosion. The H–O bond lengths and H–O–H bond angles in all of the adsorption systems are significantly different from those of a free water molecule (see Table 4), which has an H–O bond length and an H–O–H bond angle of 0.978 and 105.4°, or 0.972 and 104.8° [26], or 0.958 and 104.5° [38], indicating that the geometry of the water molecule changes notably during deposition (i.e., chemical adsorption).

In the case of water adsorption, we found that the electrode potential shift of Mo (0.065 V) was larger than that of Cr (0.035 V), which seems to suggest that the introduction of Mo leads to greater surface resistance to corrosion than that afforded by the introduction of Cr. However, chromium is generally believed to the most effective element for improving the corrosion resistance of iron-based alloy surfaces against water—even more so than molybdenum. This apparent conflict with our results can be explained as follows: although Mo is very effective at restraining interactions between the surface and adsorbed water molecules, the presence of Mo—as we noted above—also encourages the adsorption of water at the surface, which degrades its corrosion resistance properties

**Table 4** Electrode potential shifts ($\Delta U$) of different alloy surfaces upon the adsorption of oxygen or water

| Surface | Oxygen adsorption | Water adsorption | | |
|---|---|---|---|---|
| | $\Delta U$ (V) | $\Delta U$ (V) | $d_{H–O}$ (Å) | $\theta_{H–O–H}$ |
| Pure Fe | 0 | 0 | 0.994 | 106.7 |
| Fe-Cr | 0.056 | 0.035 | 0.995 | 106.9 |
| Fe-Si | 0.018 | 0.032 | 0.996 | 106.2 |
| Fe-Nb | 0.032 | −0.423 | 0.997 | 104.5 |
| Fe-Mo | 0.022 | 0.065 | 0.996 | 102.2 |
| Fe-Ti | 0.047 | −0.030 | 0.999 | 105.5 |

somewhat. Also, the solubility limit of Mo in fcc Fe is much lower than that of Cr. The good surface corrosion resistance properties of Cr derive from its tendency to discourage water adsorption and its ability to increase the surface electrode potential. Also, one of the consequences of the reaction of the surface with water would be the formation of a dense and continuous layer of $Cr_2O_3$ on the surface, which would tend to block further contact of the surface with the surrounding corrosive environment. Similarly, it is easy to see why Ti and Nb are undesirable alloying elements for improving the corrosion resistance of an fcc Fe(111) surface, as their introduction will lead to a higher adsorption energy and a lower electrode potential relative to those of the pure iron surface.

### Density of states analysis

Finally, we investigated the effects of the alloying elements on surface corrosion by analyzing the electronic structure. According to the Fermi–Dirac function, a higher Fermi energy ($E_f$) implies a lower corrosion potential. A comparison of the total densities of states (DOSs) of the different surfaces is shown in Fig. 5. For oxygen adsorption, DOS analysis suggests that $E_f$ decreases in the presence of all five alloying elements considered, and the corrosion potential decreases in the order Cr > Mo > Nb > Ti > Si. This indicates that these elements enhance the structural stability of the surface and have an inhibiting effect on surface oxidation. In the case of water adsorption, we found that the introduction of (especially) Mo or Cr or Si reduced $E_f$, but $E_f$ increased upon doping with Nb or Ti. This result indicates that introducing Cr, Si, or Mo enhances the structural stability of the surface and protects it from being corroded, whereas Nb and Ti destabilize the surface structure and degrade the corrosion resistance of the surface.

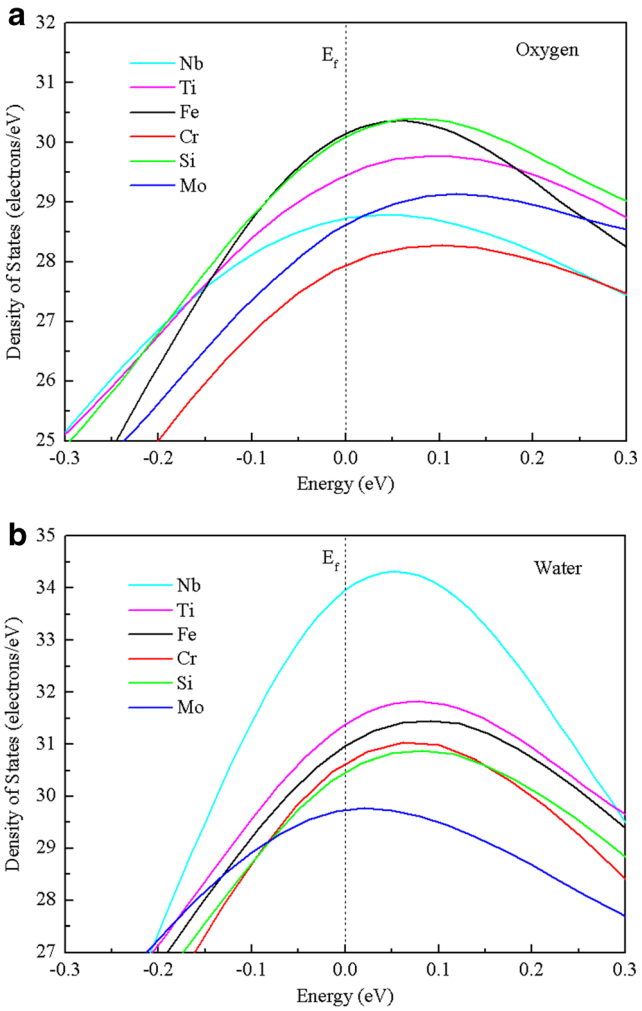


**Fig. 5** Densities of states near to $E_f$ of Fe surfaces doped with various alloying elements upon oxygen and water adsorption

## Conclusions

In summary, a first-principles investigation of the effects of ten common alloying elements (Cr, Si, Cu, Al, Ni, Nb, Co, Mo, Mn, Ti) on oxygen or water adsorption on a γ-Fe(111) surface and the electrochemical stabilities of the surfaces of the corresponding alloys was carried out. According to segregation energy calculations, all of these alloying elements have a tendency to segregate towards the γ-Fe(111) surface. Adsorption energies and electrode potentials were calculated to gauge the possibility of O or $H_2O$ adsorption on the alloy surfaces and the electrochemical stabilities of those surfaces, respectively. Upon combining the results of the effects of alloying on both adsorption and electrode potential, we found that the introduction of each of the ten alloying elements (especially Cr, Si, and Cu) considered has a beneficial effect on the oxidation resistance of the surface. Most of the alloying elements considered—especially Cr, Mo, and Si, but not Ti and Nb—can mitigate dissolution corrosion of the γ-Fe substrate in an aqueous environment. DOS analysis further indicated that introducing Cr, Si, or Mo into a γ-Fe surface will enhance its corrosion resistance, suggesting that these alloying elements act as corrosion inhibitors; this is not true, however, of Ti and Nb.

**Acknowledgments** This work was financially supported by the National Natural Science Foundation of China (nos. 51371123, 51304145), the Specialized Research Foundation of the Doctoral Program for Institution of Higher Education (nos. 20131402211003, 20131402120004), the Natural Science Foundation of Shanxi Province (nos. 2014011002-1, 2014021018-1, 2013011010-1, 2013021013-1), and the Opening Fund of State Key Laboratory of Nonlinear Mechanics.

## References

1. Ilinčev G, Kárník D, Paulovič M, Doubková A (2006) The effect of temperature and oxygen content on the flowing liquid metal corrosion of structural steels in the Pb–Bi eutectic. Nucl Eng Des 236(18):1909–1921. doi:10.1016/j.nucengdes.2006.02.003

2. Martinelli L, Balbaud-Célérier F, Terlain A, Delpech S, Santarini G, Favergeon J, Moulin G, Tabarant M, Picard G (2008) Oxidation mechanism of a Fe–9Cr–1Mo steel by liquid Pb–Bi eutectic alloy (part I). Corros Sci 50(9):2523–2536. doi:10.1016/j.corsci.2008.06.050
3. Zhang J, Li N (2005) Oxidation mechanism of steels in liquid–lead alloys. Oxid Met 63(5-6):353–381. doi:10.1007/s11085-005-4392-3
4. German E, Efremenko I (2004) Calculation of the activation energies of dissociative oxygen adsorption on the surfaces of rhodium (111), silver (111) and (110), and gold (111). J Mol Struct 711:159–165
5. Yang TT, Bi HT, Cheng XX (2011) Effects of $O_2$, $CO_2$ and $H_2O$ on $NO_x$ adsorption and selective catalytic reduction over Fe/ZSM-5. Appl Catal B Environ 102(1-2):163–171. doi:10.1016/j.apcatb.2010.11.038
6. Demetriou A, Pashalidis I (2012) Spectophotometric studies on the competitive adsorption of boric acid (B(III)) and chromate (Cr(VI)) onto iron (oxy)hydroxide (Fe(O)OH). Global Nest J 14(1):32–39
7. Bryliakov KP, Talsi EP (2014) Active sites and mechanisms of bioinspired oxidation with $H_2O_2$, catalyzed by non-heme Fe and related Mn complexes. Coord Chem Rev 276:73–96. doi:10.1016/j.ccr.2014.06.009
8. Idczak R, Idczak K, Konieczny R (2014) Oxidation and surface segregation of chromium in Fe-Cr alloys studied by Mossbauer and X-ray photoelectron spectroscopy. J Nucl Mater 452(1-3):141–146. doi:10.1016/j.jnucmat.2014.05.003
9. Chen S, Giorgi ML, Guillot JB, Geneste G (2012) Oxidation and diffusion processes at the Mn-doped Fe(001) and Fe(110) surfaces from first-principles. Appl Surf Sci 258(22):8613–8618. doi:10.1016/j.apsusc.2012.05.060
10. Jiang D, Carter E (2004) Diffusion of interstitial hydrogen into and through bcc Fe from first principles. Phys Rev B 70:064102. doi:10.1103/PhysRevB.70.064102
11. Jiang D, Carter E (2005) Carbon atom adsorption on and diffusion into Fe(110) and Fe(100) from first principles. Phys Rev B 71:045402. doi:10.1103/PhysRevB.71.045402
12. Nunomura N, Sunada S (2013) First-principles simulations of the initial corrosion process of iron surface. In: Marquis F (ed) PRICM: 8 Pacific Rim International Congress on Advanced Materials and Processing. Wiley, Hoboken
13. Zhao W, Wang JD, Liu FB, Chen DR (2009) Equilibrium geometric structure and electronic properties of Cl and $H_2O$ co-adsorption on Fe(100) surface. Chin Sci Bull 54(8):1295–1301. doi:10.1007/s11434-009-0199-y
14. Jussila P, Ali-Löytty H, Lahtonen K, Hirsimäki M, Valden M (2009) Inhibition of initial surface oxidation by strongly bound hydroxyl species and Cr segregation: $H_2O$ and $O_2$ adsorption on Fe–17Cr. Surf Sci 603(19):3005–3010. doi:10.1016/j.susc.2009.08.006
15. Błoński P, Kiejna A, Hafner J (2005) Theoretical study of oxygen adsorption at the Fe(110) and (100) surfaces. Surf Sci 590(1):88–100. doi:10.1016/j.susc.2005.06.011
16. Freitas RRQ, Rivelino R, de Brito Mota F, de Castilho CMC (2012) Dissociative adsorption and aggregation of water on the Fe(100) surface: a DFT study. J Phys Chem C 116(38):20306–20314. doi:10.1021/jp303684y
17. Xu YC, Song C, Zhang YG, Liu CS, Pan BC, Wang ZG (2014) An energetic evaluation of dissolution corrosion capabilities of liquid metals on iron surface. Phys Chem Chem Phys 16(31):16837–16845. doi:10.1039/C4cp01224k
18. Blau PJ, Brummett TM, Pint BA (2009) Effects of prior surface damage on high-temperature oxidation of Fe-, Ni-, and Co-based alloys. Wear 267(1-4):380–386. doi:10.1016/j.wear.2008.12.082
19. Nunomura N, Sunada S (2012) First-principles study of $H_2O$ adsorption on oxygen-covered Fe surface. Mater Sci Forum 706–709:1481–1484. doi:10.4028/www.scientific.net/MSF.706-709.1481
20. Tan X, Zhou J, Peng Y (2012) First-principles study of oxygen adsorption on Fe(110) surface. Appl Surf Sci 258(22):8484–8491. doi:10.1016/j.apsusc.2012.04.162
21. Yuan X-S, Song C, Kong X-S, Xu Y-C, Fang QF, Liu CS (2013) Segregation of alloying atoms on the Fe(100) surface and their effects on oxygen adsorption. Phys B Condens Matter 425:42–47. doi:10.1016/j.physb.2013.05.028
22. Zhao W, Wang JD, Lu FB, Chen DR (2009) First principles study of $H_2O$ molecule adsorption on Fe(100), Fe(110) and Fe(111) surfaces. Acta Phys Sin Chin Ed 58(5):3352–3358
23. Yu J, Lin X, Wang J, Chen J, Huang W (2009) First-principles study of the relaxation and energy of bcc-Fe, fcc-Fe and AISI-304 stainless steel surfaces. Appl Surf Sci 255(22):9032–9039. doi:10.1016/j.apsusc.2009.06.087
24. Lee S-J, Lee Y-K, Soon A (2012) The austenite/ε martensite interface: a first-principles investigation of the fcc Fe(111)/hcp Fe(0001) system. Appl Surf Sci 258(24):9977–9981. doi:10.1016/j.apsusc.2012.06.059
25. Paduani C (2005) First principles calculations of the local moments for 4d impurities in bcc and fcc iron. Mater Sci Eng B 121(1–2):9–11. doi:10.1016/j.mseb.2004.12.001
26. Kohn W, Sham LJ (1965) Self-consistent equations including exchange and correlation effects. Phys Rev 140(4A):A1133–A1138
27. Hohenberg P, Kohn W (1964) Inhomogeneous electron gas. Phys Rev 136(3B):B864–B871
28. Clark SJ, Segall MD, Pickard CJ, Hasnip PJ, Probert MIJ, Refson K, Payne MC (2005) First principles methods using CASTEP. Z Krist 220(5/6/2005):567–570. doi:10.1524/zkri.220.5.567.65075
29. Perdew JP, Zunger A (1981) Self-interaction correction to density-functional approximations for many-electron systems. Phys Rev B 23(10):5048–5079
30. Ceperley DM, Alder BJ (1980) Ground state of the electron gas by a stochastic method. Phys Rev Lett 45(7):566–569
31. Monkhorst HJ, Pack JD (1976) Special points for Brillouin-zone integrations. Phys Rev B 13(12):5188–5192
32. Jiang D, Carter E (2003) Carbon dissolution and diffusion in ferrite and austenite from first principles. Phys Rev B 67:214103. doi:10.1103/PhysRevB.67.214103
33. Basinski ZS, Hume-Rothery W, Sutton AL (1955) The lattice expansion of iron. Proc R Soc Lond A Math Phys Sci 229(1179):459–467. doi:10.1098/rspa.1955.0102
34. Häglund J, Fernández Guillermet A, Grimvall G, Körling M (1993) Theory of bonding in transition-metal carbides and nitrides. Phys Rev B 48(16):11685–11691
35. Zhong W, Overney G, Tománek D (1993) Structural properties of Fe crystals. Phys Rev B 47(1):95–99. doi:10.1103/PhysRevB.47.95
36. Moruzzi VL, Marcus PM, Schwarz K, Mohn P (1986) Ferromagnetic phases of bcc and fcc Fe, Co, and Ni. Phys Rev B 34(3):1784–1791. doi:10.1103/PhysRevB.34.1784
37. Macdonald F, Lide DR (2003) CRC handbook of chemistry and physics: from paper to web. Abstr Pap Am Chem Soc 225:U552
38. Lü B-L, Chen G-Q, Zhou W-L, Su H, Liu R (2011) Ab initio study of influence of 3d alloying elements on corrosion properties of non-passivated nickel-base alloys. J Nucl Mater 418:286–291. doi:10.1016/j.jnucmat.2011.07.015
39. Kiejna A, Wachowicz E (2008) Segregation of Cr impurities at bcc iron surfaces: first-principles calculations. Phys Rev B 78:113403. doi:10.1103/PhysRevB.78.113403
40. Gupta M, Gupta RP (2013) Anomalous surface segregation behaviour of some 3d elements in ferromagnetic iron. J Phys Condens Matter 25:415502. doi:10.1088/0953-8984/25/41/415502
41. Levesque M (2013) Anomalous surface segregation profiles in ferritic Fe-Cr stainless steel. Phys Rev B 87:075409. doi:10.1103/Physrevb.87.075409

42. Levesque M, Gupta M, Gupta RP (2012) Electronic origin of the anomalous segregation behavior of Cr in Fe-rich Fe-Cr alloys. Phys Rev B 85:064111. doi:10.1103/Physrevb.85.064111
43. Ponomareva AV, Isaev EI, Skorodumova NV, Vekilov YK, Abrikosov IA (2007) Surface segregation energy in bcc Fe-rich Fe-Cr alloys. Phys Rev B 75:245406. doi:10.1103/PhysRevB.75.245406
44. Greeley J, Nørskov JK (2007) Electrochemical dissolution of surface alloys in acids: thermodynamic trends from first-principles calculations. Electrochim Acta 52(19):5829–5836. doi:10.1016/j.electacta.2007.02.082
45. Ma YG, Balbuena PB (2008) Surface properties and dissolution trends of $Pt_3M$ alloys in the presence of adsorbates. J Phys Chem C 112(37):14520–14528. doi:10.1021/Jp8046888